



Characterization and efficient dye discoloration of Algerian diatomite from Ouled Djilali-Mostaganem

Amal Touina^{1,2} · Safia Chernai^{1,2} · Bouhameur Mansour³ · Hafida Hadjar⁴ · Abdelkader Ouakouak⁵ · Boualem Hamdi^{1,2}

Received: 16 November 2020 / Accepted: 3 February 2021 / Published online: 20 March 2021
© The Author(s) 2021

Abstract

A series of naturally occurring diatomaceous earth samples from Ouled Djilali, Mostaganem (Lower Chelif basin, Algeria northwestern), were investigated, which are characterized by the expansion and evolution during the Messinian age. Four varieties of diatomite were distinguished, characterized, and successfully used to adsorb methylene blue dye in aqueous medium. Several properties and characteristics of diatomite have been outlined using analytical methods such as X-ray fluorescence spectrometry, X-ray diffraction (XRD), Fourier transform infrared spectroscopy (FTIR), N₂ adsorption–desorption (BET), and scanning electron microscopy (SEM), as well as other complementary analysis tests. Results showed that silica and calcium carbonates were the main constituents of the diatomite samples (ranging between 32.8 and 61.5% for SiO₂; and 13.8–25.9% for CaO), with a slight difference in chemical composition between selected samples. Typical for all diatomite samples, the XRD analysis suggests a high mass quantity of amorphous phase (Opal); high content of crystal phase was also registered. FTIR allowed determining the basic characteristic silica bands regarding diatomite samples. While the BET and SEM investigations revealed that the studied diatomite material has a highly porous structure and was very rich in diatoms. The maximum adsorption capacity of methylene blue that was calculated from the Langmuir isotherm model was 116.59 mg/g (for Ouled Djilali: OD05 sample) at 25 °C and pH 7.0. The diatomite from Mostaganemian (Ouled Djilali) deposit may find promising applications as low-cost adsorbent for dyes removal from water.

Keywords Diatomite · Characterization · Adsorption · Methylene blue · Isotherm model

1 Introduction

Nowadays, water pollution has given rise to serious environmental problems [1]. Among the different contaminants affecting the aquatic ecosystems, dyes belong to one of the larger and most important groups generally discharged in wastewaters from industrial and agricultural sectors, which present considerable toxicity to human beings and living organisms [2]. Hence, the depollution

of water from dyes has become of high priority concern. In response, several methods have been studied to assess their applicability and removal efficiency. Among these methods, adsorption especially onto activated carbon has been considered as the most effective and widely used one [3–7]. Nevertheless, due to the expensive price and difficult regeneration process of activated carbons, worldwide attention has been focused on finding out alternative adsorbents such as bentonite [8], waste sludge [9], maine

✉ Amal Touina, amaltouina@yahoo.com | ¹Laboratoire de Conservation et de Valorisation des Ressources Marines (LCVRM), Algiers, Algeria. ²Ecole Nationale Supérieure des Sciences de la Mer et de l'Aménagement du Littoral (ENSSMAL), Campus Universitaire, Bois des Cars, Dely Ibrahim, BP 19, Algiers, Algeria. ³Laboratoire de Paléontologie Stratigraphique et Paléoenvironnements (LPSP), Université D'Oran 2 Ahmed Ben Ahmed, Oran, Algeria. ⁴CRAPC, Centre de Recherche Scientifique et Technique en Analyses Physico-Chimiques, Zone Industrielle, RP, BP 384, 42004 Bou-Ismaïl, Tipaza, Algeria. ⁵Hydraulic and Civil Engineering Department, University of El Oued, El Oued, Algeria.



algae (*Ulva lactuca* and *Sargassum*) [10], bagasse fly ash [11], and almond peel [12].

Diatomite, otherwise known as kieselguhr, diatomaceous earth (DE), or “Tripoli” of Sicily, is provided from the Messinian diatomitic formation [13]. It represents one of the most significant sedimentary events of the Neogene in the Mediterranean [14]. Diatomite is a silica rock consisting essentially of fossilized skeletal remains of single-celled aquatic algae called diatoms. It is characterized by the presence of a rigid skeleton made of hydrated silica (opal), called frustule [15], with a number of impurities such as inorganic and organic matters, and even clay minerals [16]. There are nearly 10,000 species of diatoms forming vast deposits of sedimentation in various parts of the earth. Due to its unique advantages and desirable properties, high porosity and small particle size, that give to the diatomite low density, high permeability, high adsorption capacity and specific surface area, and low thermal conductivity [17], the diatomite provides a wide variety of uses in sustainable development and environment such as purification of drinking water, filtration, insulation, adsorption, manufacture of antibiotics, catalysis, and as an additive in cement [18–20].

Algeria is considered to have rich area of natural DE deposits situated in a wide basin called Lower Chelif Basin. These deposits are still little exploited, since the most important exploitation is mainly concentrated on the site of Sig in western Algeria. The present contribution aims to first highlight the physicochemical, mineralogical and textural properties of a natural diatomite from the Mostaganemian deposit (Ouled Djilali) using various methods: X-ray fluorescence spectrometry (XRF), X-ray diffraction (XRD), scanning electron microscopy (SEM), Fourier transform infrared spectroscopy (FTIR), and N_2 -BET (Brunauer, Emmett, and Teller) adsorption–desorption technique. Adsorption tests were thereafter conducted on the as-studied material to explore on the removal process efficiency of a cationic dye (methylene blue) from aqueous media. Different isotherm models were examined for analyzing the equilibrium data and for a better understanding of the adsorption process.

2 Location and reserves of Lower Chelif Basin diatomite deposits

2.1 Lower Chelif Basin

The current area of interest occurs along the northeastern border of the Lower Chelif Basin; in the northwestern region of Algeria is part of the Lower Chelif Basin (Fig. 1). The basin is regarded as the largest intramountainous basin in the north of Algeria [21], in the same way as the large marginal Neogene basins of the Mediterranean [22].

Geomorphologically, it is a long depression (ENE/WSW direction) over about 350 km and 35 km wide. It is limited to the north by the Oranean coast (Djebel Murdjadjo, Arzew mountains) and Dahra mountains. Tessala, Beni Chougrane, Ouled Ali, and Ouarsenis Mounts represent its borders to the South.

2.2 Ouled Djilali sampling area

The selected diatomite sampling area is deposited in Ouled Djilali location southeastern part of Daira of Sidi Ali, throughout a distance of 11.92 km (N: 36°, 02', and 36.2". E: 000°, 31', 44.4"). It is bounded on the north by Douar Gouassmia, Jebel Chaif Dahmane, and Douar El B'Hara, in the south by Douar Ouled Fellouh, and Douar Ouled Mokhtar, in the east by Douar Haddou, and in the west by Douar Soualmia and Douar Torche (Fig. 2).

3 Materials and methods

3.1 Preparation of samples

Four varieties of natural diatomite samples taken from each layer from the deposit of Ouled Djilali have been distinguished on the basis of the colors variability of the diatomite rocks, their structural and textural features, and their fracturing effects (Table 1; Fig. 3). The samples were denoted with the letters OD (according to the site name: Ouled Djilali), with additional numbers that correspond to the different layers.

The OD samples employed in this study were first dried at a temperature of 110 °C overnight. After being crushed in HERZOG grinder in a tungsten bowl (3 min at 700 rpm), the samples were sieved to obtain a size fraction of 63 μm (no refusal must remain) for characterization with X-ray diffraction and X-ray fluorescence methods, while a size fractions between 100 and 200 μm , served to allow easier analysis.

3.2 Characterization

The chemical compositions of the raw material were determined by X-ray fluorescence spectroscopy (XRF) (S8 TIGER de Bruker). X-ray powder diffraction data (XRD) were acquired with a BrukerD4 ENDEAVOR analyzer operating with a $\text{CuK}\alpha$ radiation source filtered with a graphic monochromator $\lambda = 1.5406 \text{ \AA}$. The surface morphology of the raw samples was illustrated by scanning electron microscopy (SEM), using « Philips XL 30 model ESEM-FEG» operating at 8 kV. The Fourier transform infrared (FTIR) spectra were obtained from a «Perkin Elmer» spectrometer

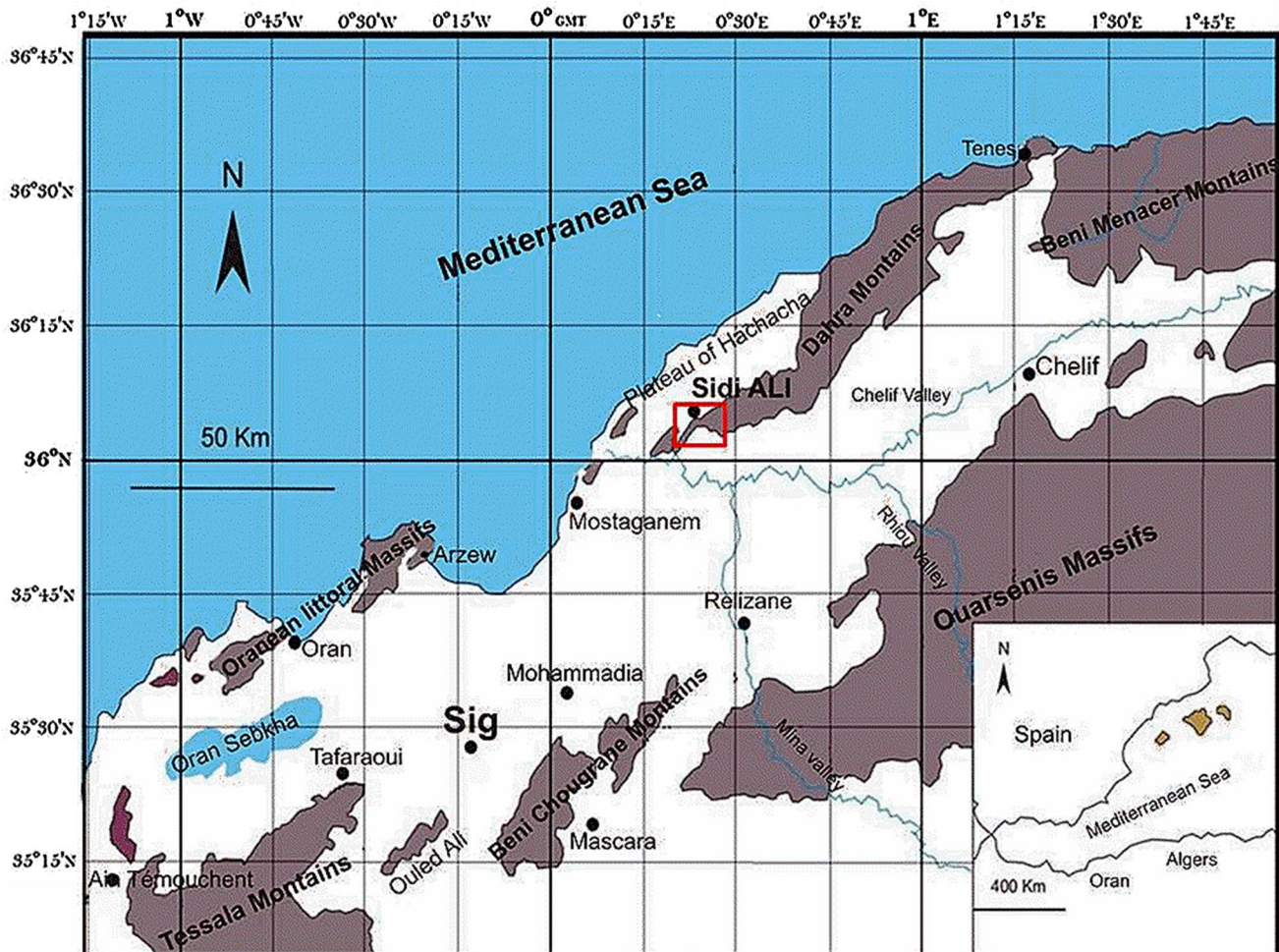


Fig. 1 Location of the studied site in the Lower Chelif Basin (Algeria) (CorelDRAW 12)

connected to a computer with the scanning range from 400 to 4000 cm^{-1} .

The characterization of the specific surface area and Brunauer, Emmett and Teller (BET) texture parameters of Ouled Djilali diatomite was carried out by low-temperature adsorption of nitrogen (at 77.3 K) using a Micromeritics ASAP-2420 surface area analyzer. The degassing of the diatomite samples was performed for 12 h at a heating temperature of 140 °C. The nitrogen adsorption–desorption isotherms were analyzed to evaluate the required parameters; the specific surface areas (S_{BET}) were determined on the basis of the BET equation. The total pore volume (V_t) was estimated in accordance with the rule of Gurvich at a relative pressure of 0.977. The volume of the mesopores (V_{mes}) was evaluated from the difference between the total pore volume (V_t) and that of the micropores (V_{mic}).

3.3 Physicochemical properties

In this part, the diatomite samples were first crushed and sieved at 200 μm . Several physicochemical parameters were studied. For pH determination, diatomite suspensions (2 g of sample in 100 ml of ultrapure water) were prepared in a beaker of 200 ml volume. The mixtures were stirred for 6 h, and the pH of the aqueous solutions was measured immediately on a pH meter model Hi 208, Hanna instruments. For the chloride ion percentage, diatomite suspensions (1 g of diatomite in 75 ml of ultrapure water) were boiled until a volume of 50 ml. After cooling, the content was filtered, and the chlorides percentage was estimated by MOHR's method (argentometric method) using silver nitrate as titrant and potassium chromate as indicator solution. The apparent density was expressed by means of the ratio between the mass of diatomite (g) and

the occupied volume (cm³). The percentage of humidity was estimated by lyophilization process of the samples for 48 h.

Regarding the water and oil adsorption rate, the determination of their values was obtained by calculation of the ratio between the maximum amount of oil (sunflower oil), or water adsorbed on the diatomite and its mass.

3.4 Batch adsorption experiment

The process of methylene blue (MB) dye removal was conducted under common batch adsorption experiments. Approximately, 0.1 g of the natural Ouled Djilali diatomite was put in contact with 50 mL of MB dye solution at different desired concentrations (10, 20, 30, 40, 50, 80, 120, 160, and 200 mg/L). Each adsorbent–adsorbate mixture was mechanically stirred at 125 rpm at ambient temperature (25 °C) until it reached the adsorption equilibrium (according to preliminary results, the contact time was fixed to 60 min). Following this, a 0.45 μm membrane filter was used to separate each dye solution from the corresponding dye–diatomite interaction system. The residual concentration in the MB supernatant was analyzed using a UV–Vis spectrophotometer at the wavelength λ_{max} = 665 nm. All adsorption tests were performed at

pH = 7.0. The solutions involved were diluted to proper concentrations before making measurements. The quantity of adsorbed MB at equilibrium (q_e, mg/g) was calculated as follows:

$$q_e = (C_0 - C_e) * V/m \tag{1}$$

where C₀ and C_e (mg/L) are the concentration of MB ions at the beginning and the equilibrium concentration, respectively. V(L) is the volume of MB solution, whereas m (g) represents the mass of diatomite adsorbent.

Regarding the modeling of the adsorption isotherm, Langmuir, Freundlich, Sips and Temkin isotherm models are well applied to describe the adsorption process. More detailed information and derivation of such models are summarized in Table 2.

4 Results and discussion

4.1 Macroscopic properties

The whitish raw OD diatomite material has a laminated structure with fine grains, releasing easily in hand. It can be scratched with no significant resistance. Whereas the



Fig. 2 Geographical location of the Ouled Djilali sampling area (N: 36°, 02', 36.2". E: 000°, 31', 44.4") (ARCGIS)

Table 1 Macroscopic description of natural diatomite samples from deposit of Ouled Djilali

Sample	Nature	Color	Features and fracturing effects
OD03	Diatomite	Whitish	Laminated, light, pulverous
OD04	Diatomite	Whitish	++ Laminated, light, pulverous
OD05	Marly diatomite	Beige	Indurate, massive
OD08	Marly diatomite	Beige	++ Laminated, pulverous

+ More



Fig. 3 Panoramic view of the studied site

darker samples are massive, indurate, and highly resistant, this required the use of a big grinding material (HERZOG grinder). They can be also laminated and easily crumbled in hand. The raw material is a lightweight sedimentary rock having strong water absorbability, which emphasizes a high porosity. Because the sampling was done during a rainfall period, the samples contained a large volume

of water; significant time was thus required to release absorbed water from samples.

4.2 Geochemical composition by XRF

The geochemical composition of the natural OD diatomite samples was obtained by the X-ray fluorescence spectroscopy, expressed by means of weight percentages, as reported in Table 3. Loss-on-ignition represents the percentage of material removed during the air calcination of a sample at 950°C. As can be seen, the XRF results depict that the main components of the raw OD diatomite consist of silica (SiO₂), with significant amounts of calcium (Ca) being mainly in the form of carbonate, whereas other mineral components, existing typically as impurities in minor amounts, contribute to the rest of the diatomite composition. Although the raw diatomite samples are located in the same deposit, the XRF results show significant differences in the SiO₂ and CaO percentages between samples, in contrary of the other admixtures contents. The whitish raw materials are composed of 49.5–61.5% SiO₂, except for the indurate marl-diatomite (sample OD5) that contains only 32.8% SiO₂. The CaO content varies from 13.8 to 25.9% which generally does not depend on the diatomite variety distinguished on the base of the variability of rock colors, and textural features, as it is with the SiO₂ content. The two OD04 and OD05 samples have the most elevated value of loss on ignition (LOI). They represent the darker colored diatomite varieties, and both their features (LOI and color) depend probably upon the presence of high amount of organic substances. Indeed, we notice in Table 3 that the rate in LOI is correlated with the rate in CaO (as aforementioned, Ca exists in the natural diatomaceous earth product as calcium carbonate (CaCO₃) which decomposes into CaO and CO₂ above 800 °C). The presence of high content of SiO₂ in both OD03 and OD04 diatomite

Table 2 Equations and relevant parameters of the used isotherm models

Isotherm models	Equation	Description parameters	References
Langmuir	$q_e = \frac{Q_{max}^0 K_L C_e}{1 + K_L C_e}$	C_e : concentration of MB dye at equilibrium Q_{max}^0 (mg/g): maximum monolayer adsorption capacity of Langmuir	[23]
Freundlich	$q_e = K_F C_e^n$	K_L (L/mg): Langmuir constant	[24]
Sips	$q_e = \frac{Q_{max}^0 K_S C_e^{1/ns}}{1 + K_S C_e^{1/ns}}$	C_0 (mg/L): initial MB dye concentration K_F [(mg/g)/(mg/L) ⁿ]: Freundlich constant n : dimensionless Freundlich intensity parameter	[25]
Temkin	$q_e = \frac{R \cdot T}{\Delta Q} \cdot \ln(K \cdot C_e)$	Q_{max}^0 (mg/g): the Sips maximum adsorption capacity K_S (mg/L) ^{-1/n} : the Sips equilibrium constant n : the exponent of Sips where $0 < 1/ns \leq 1$ ΔQ (J/mol): the heat transfer R ($R = 8.314$ J/mol/K): the universal gas constant T (K): the temperature	[26]

Table 3 Geochemical composition of the natural diatomite samples of Ouled Djilali section (in Weight (%))

Samples	OD03	OD04	OD05	OD08
SiO ₂	61.52	58.9	32.8	49.5
Al ₂ O ₃	3.88	3.55	5.7	3.44
Fe ₂ O ₃	1.66	1.5	2.26	1.53
CaO	13.8	15.2	25.9	21.7
MgO	1.53	1.42	3.14	0.4
SO ₃	0.1	0.1	0.15	0.12
K ₂ O	0.84	0.79	0.49	0.7
Na ₂ O	0.21	0.22	1.26	0.32
P ₂ O ₅	0.05	0.06	0.07	0.07
TiO ₂	0.19	0.18	0.29	0.17
Cr ₂ O ₃	0.006	0.005	0.007	0.005
Mn ₂ O ₃	0.012	0.013	0.022	0.025
ZnO	0.004	0.004	0.005	0.004
SrO	0.05	0.05	0.09	0.08
LOI (950 °C)	15.85	20.69	27.53	17.20

LOI loss on ignition

samples make them interesting materials for adsorption in various.

4.3 XRD analysis

XRD analysis was performed on OD natural diatomite samples for mineralogical and chemical identifications, and the corresponding diagrams are shown in Fig. 4. Additionally, the X-ray detailed diffraction peaks information is listed in Table 4. Typical for all samples and more specifically for OD04 and OD08 materials, the specific shape of the obtained diffractograms and the high intensity of the background suggest a high mass quantity of SiO₂ present as amorphous opal A phase whose reflections dominate in the corresponding XRD patterns between 19° and 32° (2 Theta), this finding being in accordance with the XRF results. A high content of crystalline phase and the most important reflections corresponding to calcite, dolomite, illite, and kaolinite phases are also observed (Table 4)

Fig. 4 XRD patterns of the diatomite samples of Ouled Djilali (Q: quartz, C: calcite, D: dolomite, A: alumina)

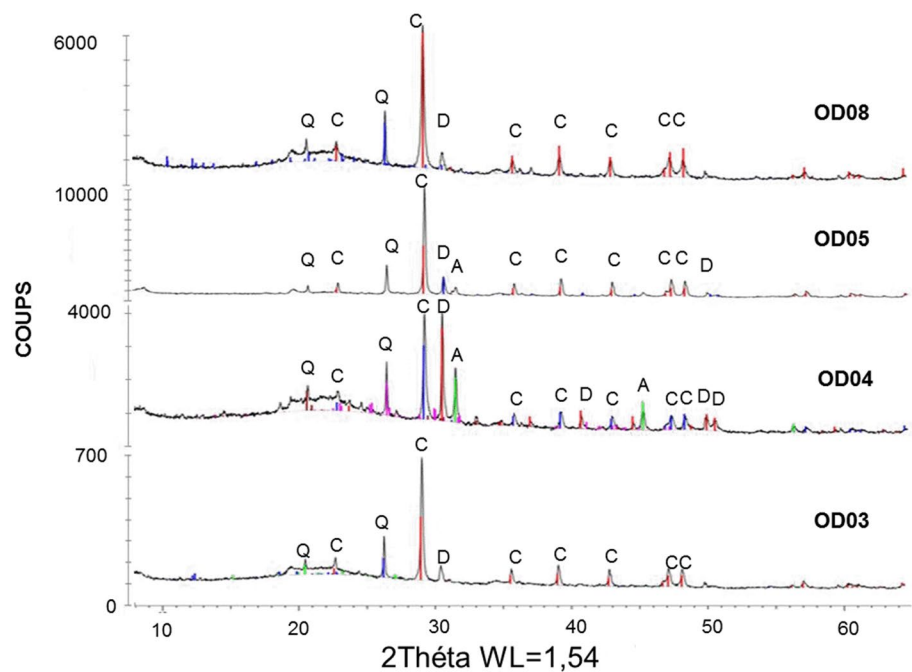


Table 4 Mineral phases (%) of the Ouled Djilali diatomite samples

Samples	Calcite	Dolomite	Quartz	Pyrite	Illite	Chlorite	Kaolinite	Albite
OD03	47.54	6.66	7.03	–	19.26	–	13.82	5.69
OD04	33.96	24.4	4.66	0.15	18.34	2.33	13.78	2.36
OD05	55.72	8.69	6.61	–	20.25	1.81	4.78	2.13
OD08	49.10	7.16	5.76	–	17.79	–	14.26	5.93

revealing raw materials with irregular structures. The difference in impurities contents such as albite, chlorite, and pyrite also points to the different sedimentary environments of the diatomite samples.

4.4 SEM analysis

An insight was provided about the morphology and microstructure of the obtained OD diatomite samples by means of scanning electron microscopy (SEM) characterization. The microscopic pictures revealed the existence of intact diatomite skeletons whose framework structure is composed of diatomite shells represented by various diatom morphological types. The SEM observation clearly confirmed the presence of a well-defined and mostly preserved porous structure, which is an important parameter and key medium for any adsorption process, the porous shells consisting mainly of SiO_2 groups [27, 28]. It can be also inferred that the diatomite samples are rich in two classes of diatoms: centric and pennate, and large void volumes (Fig. 5a–c). Each frustule of diatom contains areolae due to its high porosity, and the size and disposition of these areolae vary with the species nature. The high porosity of the studied diatomite material was one of the main reasons for selecting it as a potential sorbent.

4.5 Fourier transform infrared spectroscopy (FTIR)

FTIR technique was used to confirm the presence of the functional groups of the diatomite before their use as dye adsorbent. The FTIR analyses spectra are gathered in Fig. 6. There are no significant differences between the positions of the basic characteristic bands. Based upon reviewing the analysis data, the characteristic peaks of diatomite are clearly detected at 3435 , 1426 , 1070 , 800 and 454 cm^{-1} . The band at 3435 cm^{-1} is due to stretching vibration of the hydroxyl groups in physically adsorbed water molecules (silanol group SiO-H) [29–31], and this group is responsible for the adsorption process [32]. The carbonates IR band appears at 1426 cm^{-1} [33]. The rocking and asymmetric stretching vibration band of siloxane ($-\text{Si-O-Si}-$) in diatomite appears at wave numbers 1070 cm^{-1} [30, 33, 34]. Other bands at 800 and 454 cm^{-1} are also characteristic of silica; the first one may be related to the stretching vibration of Al-O-Si [35], but it can be also attributed to O-H deformation or the free silica and/or symmetric stretching in SiO-H [31, 36, 37], whereas the second band is assigned to the bending vibrations of Si-O-Si [36].

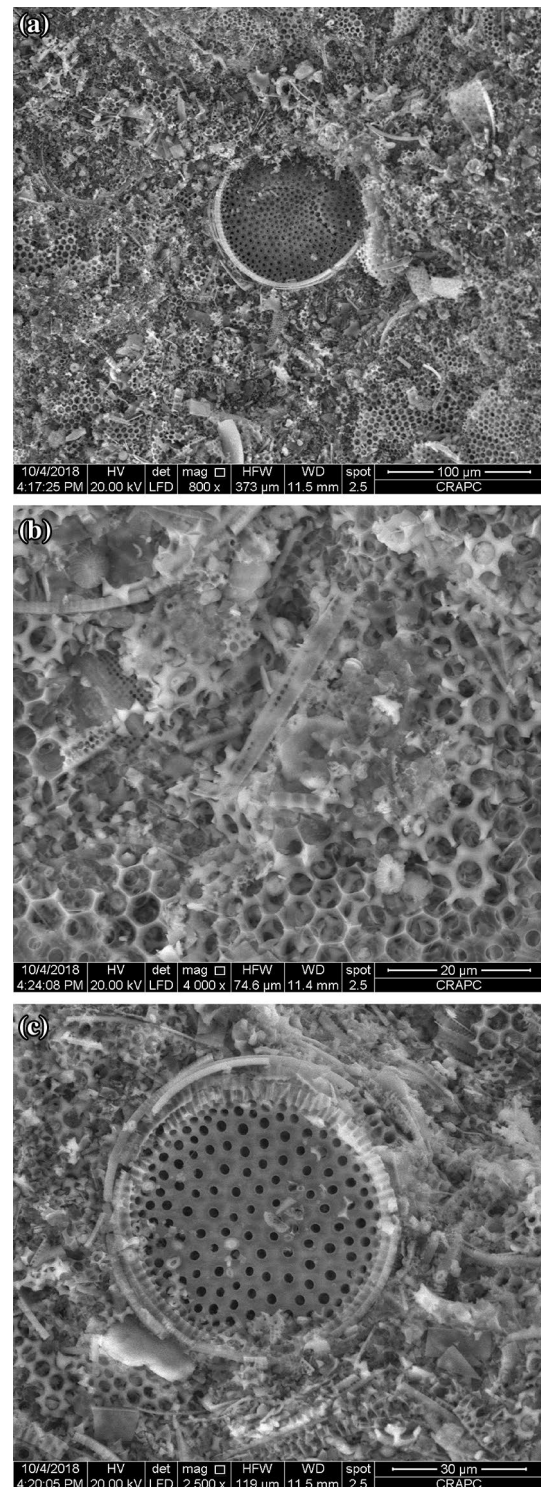


Fig. 5 **a** Morphology observed with SEM images of OD03 diatomite sample. **b** Morphology observed with SEM images of OD03 diatomite sample. **c** Morphology observed with SEM images of OD03 diatomite sample

Fig. 6 FTIR spectra of the diatomite samples of Ouled Djilali

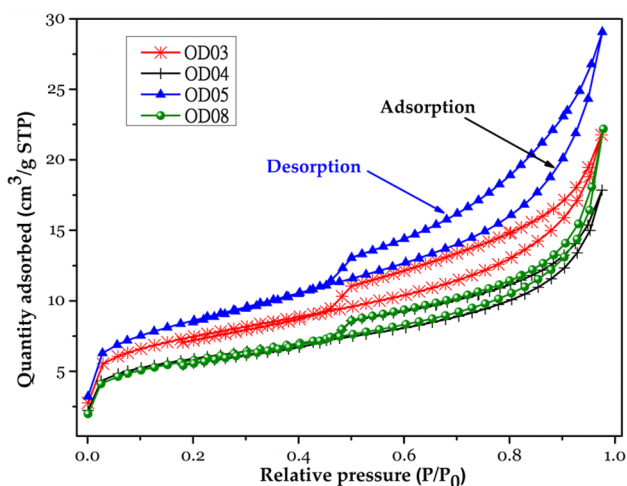
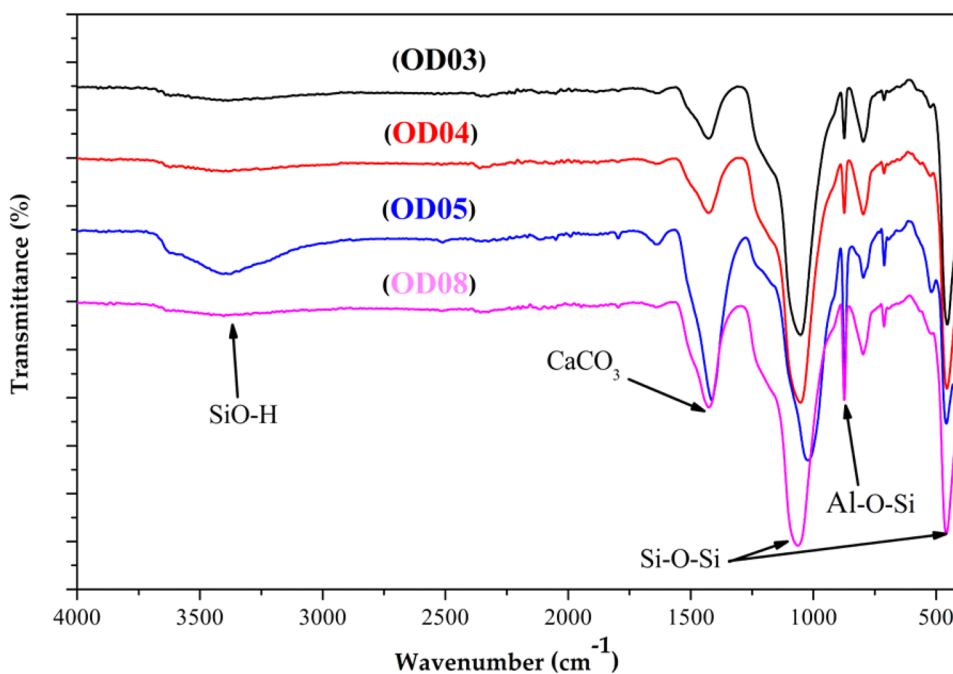


Fig. 7 Nitrogen adsorption–desorption isotherms of raw diatomite samples of Ouled Djilali

Considering these functional groups on the surface of the diatomite which facilitate the electrostatic attraction with the cationic MB, it is proposed that hydrogen bond would be formed between the raw diatomite and MB and contributes significantly to the high adsorption of dye [27].

4.6 N₂-sorption study

The N₂ adsorption–desorption isotherms of the studied OD diatomite at liquid nitrogen temperature are provided in Fig. 7. BET and external surface areas as well as pore volumes of the diatomite samples calculated on the basis of these isotherms are summarized in Table 5. As shown in Fig. 7, all the raw OD diatomite samples present the same Type IV nitrogen adsorption–desorption isotherm shape, exhibiting a characteristic feature as type II isotherms in addition to a steep uptake at P/P₀ of above 0.8 which can be assigned to the existence of macropores in the raw

Table 5 Textural parameters of the natural diatomite samples of Ouled Djilali

Samples	V _t (cm ³ /g) NTU	V _{mes} (cm ³ /g)	V _{mic} (cm ³ /g)	S _{BET} (m ² /g)	S _{ext} (m ² /g)
OD03	0.034	0.028	0.006	58.87	3.99
OD04	0.028	0.023	0.005	45.28	2.98
OD05	0.045	0.040	0.005	69.95	5.38
OD08	0.034	0.030	0.004	47.91	3.31

V_t, total pores volume; V_{mes}, mesoporous volume, V_{mic}, microporous volume, S_{BET}, BET area, S_{ext}, external surface area

Table 6 Physicochemical and textural characteristics of diatomite materials

Diatomite from	SiO ₂ %	CaO %	S _{BET} (m ² /g)	V _{total} (cm ³ /g)	V _{micro} (cm ³ /g)	pH	References
Egypt (Kom Osheam)	74.20	10.58	10–30	–	–	7.0–8.0	[39]
Awinate (Morocco)	87.71	0.4	22.7	–	–	7	[40]
Ras Traf, Rif (Morocco)	72.8	5.86	21	0.035	0.0024	-	[41]
Jordan	72	1.48	27.80				[42]
Egypt (Masakheet)	61.65	21.27					[43]
Sig (Mascara- Algeria)	67.3	19.5	22	1.4	–	7.9	[16]
Ouled Djilali	32.8–61.52	13.8–25.9	45.28–69.95	0.028–0.045	0.004–0.006	7.82–8.14	In this study

V_t, total pores volume; V_{micr}, microporous volume; S_{BET}, BET specific surface area

Table 7 Physicochemical properties of natural diatomite samples of Ouled Djilali

Samples	pH	da(*) g.cm ⁻³	H (%)	Ads H ₂ O (%)	Ads Oils (%)	Chlorides (%)
OD03	8.01	0.48	97.20	37.82	63.85	0.209
OD04	7.99	0.42	96.60	45.45	62.77	0.105
OD05	7.82	0.64	90.46	15.89	98.31	2.144
OD08	8.14	0.49	96.35	32.33	62.88	0.248

(*) da: bulk density

material. By comparing the different samples of OD diatomite, it is obvious that the OD05 has the larger BET surface area value (69.95 m² g⁻¹), which was expected to enhance the adsorption performance [38]. Besides, the Ouled Djilali diatomite (47.91–69.95 m²/g) exhibits a higher S_{BET} surface area value when compared to other diatomite materials from the literature, as shown in Table 6, and can be considered as a potential adsorbent for pollutants removal from wastewater, and environmental remediation.

4.7 Physicochemical tests

The following physical properties of OD diatomite samples have been determined in terms of apparent density (da); humidity (H), water and oil absorption (Ads H₂O, Ads Oils), and chlorides percentage. The corresponding results are summarized in Table 7.

Based on the above results, the bulk density values range from 0.42 to 0.64 g/cm³. Water absorption values are between 15.89 and 45.45%, and the oils absorption values vary from 62.77 to 98.13%. The OD04 sample has the highest average water absorption, and the lowest bulk density (light-colored diatomite). However, the darkest-colored diatomite (OD05, OD08) has the lowest water absorption and highest bulk density. The two parameters show reversely proportional dependence [42]. In contrast, the values of oil absorption and the bulk density show proportional dependence.

The pH of the diatomite aqueous suspensions lies between 7.82 and 8.14, which may be related to the

presence of alkaline oxides in the diatomite samples providing a neutral or slightly alkaline reaction of their aqueous suspensions [39].

4.8 Discoloration capacity

After examining the textural, structural and physicochemical properties of the OD diatomite powders, which significantly affect their behavior in environmental applications, these samples were subjected to a discoloration study in order to evaluate their adsorption performance by means of methylene blue (MB) dye ions recovery tests from aqueous solution, and to explore the adsorbent–adsorbate interactions. Adsorption isotherm (Fig. 8) was obtained by varying the MB initial concentration at a fixed temperature (25 °C), with maintaining a constant dose of adsorbent, the solid/liquid ratio kept at 2.0 g/L. The adsorption isotherm was categorized as an L-shape according to the Giles et al. classification [44] which suggests that the studied OD diatomite samples exhibit a high adsorption affinity toward the MB dye in solution without major competition from water molecules for the solid active sites [45]. The nonlinear forms of Langmuir, Freundlich, Sips and Temkin models were used to more interpret the obtained data and to make it easier to understand the adsorption mechanism (Fig. 8a–d). According to the isotherm constants and parameters presented in Table 8, it can be noticed that the Langmuir and Sips equations are more suitable than the Freundlich and Temkin equations for the adsorption system studied in this work. The finding regarding the

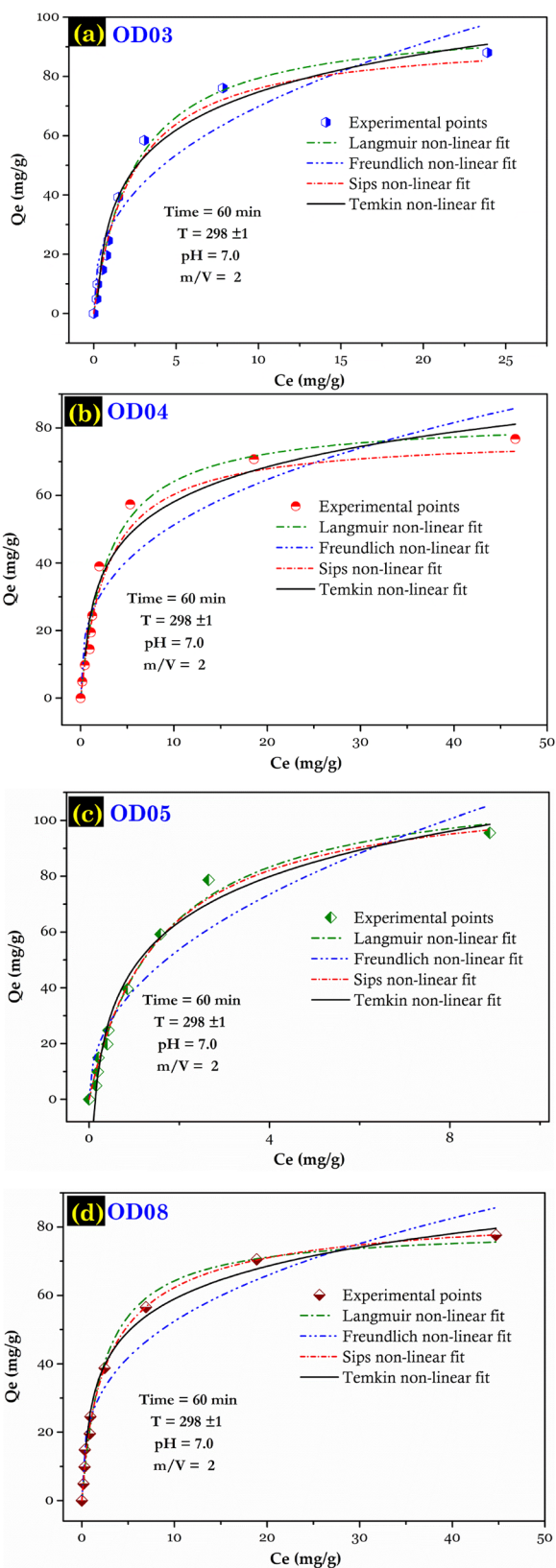


Fig. 8 Adsorption isotherm of MB onto Ouled Djilali diatomite samples (experimental conditions: $C_0 = 10\text{--}200$ mg/L, $pH = 7.0$, $m/V = 2.0$ g/L, and $t = 60$ min, $T = 25$ °C)

Langmuir fitting can be attributed to the homogenous distribution of active sites on the diatomite surface [46]. This suggests that the adsorption process of MB dye onto diatomite surfaces is favorable and monolayer in nature over the whole range of tested concentrations, induced by homogeneous solid surface energy along with no interaction between adsorbed species.

From the Langmuir model, a reasonably good maximum adsorption capacity of the studied OD diatomite samples was obtained ranging between 79.66 and 116.59 mg/g. As expected, OD05 sample exhibited the higher Q_{max}^o (116.59 mg/g) value than the other Ouled Djilali diatomite adsorbents. Obviously, adsorption efficiency is greatly related to S_{BET} and to the total volume registered values (Table 5), whereas the enhancement of these two parameters contributes to the enhancement of the adsorption capacity of the MB dye [28].

As diatomite is a natural material, it must be compared with other natural materials such as zeolite, phosphor, gypsum, clay, and other siliceous adsorbents. Table 9 shows the comparison of the adsorption capacities of some adsorbents. It is clear from the comparison that the OD05 (116.59 mg/g) possesses a higher adsorption capacity than other reported adsorbents, after the Jordanian diatomite (198 mg/g). This is probably due to the fact that the diatomite surface can interact with MB in different ways; (1) electrostatic attraction, (2) chemical adsorption via conjugation, hydrogen bonding, and pore filling mechanism [27]. It seems that the amount of MB dye loaded on the diatomite surface depends on the nature of the surface (determined by the mentioned method: FTIR, SEM, BET), which varies from a sample to another (S_{BET} , V_t and the silica percentage).

5 Conclusions and suggestions

In this study, representative raw diatomite samples were collected from Ouled Djilali (OD), Mostaganem (Lower Chelif basin, Algeria northwestern), and subjected to characterization by several methods. Results show that the silica (SiO_2) constitutes the major component of the OD diatomite with a significant amount of carbonate (CaO) beside other minor constituents.

As crystalline phases, were obtained the main accompanied minerals: calcite, dolomite, illite, and kaolinite, with less important presence of pyrite, chlorite, and albite. An interesting texture with relatively good surface area and pore volume was estimated for the studied diatomite products, along with a porous framework structure rich in intact diatom frustules (centric and pennate forms). All samples showed a high sorption capacity for oils and water.

Table 8 Parameters of adsorption equilibrium isotherms of MB dye onto diatomite samples

Model	Unit	OD03		OD04		OD05		OD08		
		Value	SD	Value	SD	Value	SD	Value	SD	
Langmuir										
Q°_{max}	mg/g	99.12	2.845	82.91	3.202	116.59	5.388	79.66	2.265	
K_L	L/mg	0.404	0.032	0.342	0.041	0.625	0.071	0.418	0.042	
R^2	–	0.994	–	0.984	–	0.988	–	0.991	–	
χ^2	–	6.078	–	12.01	–	12.47	–	6.803	–	
Freundlich										
K_F	(mg/g)/(mg/L) ⁿ	28.78	3.688	23.75	3.652	39.34	3.981	24.68	2.742	
n	–	0.385	0.052	0.334	0.051	0.451	0.059	0.327	0.037	
R^2	–	0.904	–	0.883	–	0.905	–	0.939	–	
χ^2	–	90.96	–	90.49	–	102.33	–	47.12	–	
Sips										
Q_{max}	mg/g	93.66	6.499	77.57	7.116	112.99	10.161	86.49	4.049	
K_s	L/mg	0.429	0.057	0.349	0.061	0.665	0.132	0.386	0.034	
R^2	–	0.988	–	0.971	–	0.986	–	0.995	–	
χ^2	–	11.68	–	22.38	–	15.14	–	4.03	–	
Temkin										
K_T	L/mg	5.644	0.912	4.932	1.175	7.557	0.795	7.223	0.877	
ΔQ	KJ/mol	133.71	8.595	166.20	13.471	105.73	5.339	179.81	6.944	
R^2	–	0.969	–	0.951	–	0.981	–	0.989	–	
χ^2	–	28.99	–	37.53	–	20.64	–	8.54	–	

SD, standard deviation

Table 9 Comparison of Langmuir maxima adsorption capacity (Q°_{max}) of MB dye

	Textural properties		Adsorption isotherm condition				Q°_{max} (mg/g)	References
	S_{BET} (m ² /g)	V_{total} (cm ³ /g)	pH	Time (h)	C_0 (mg/L) range	T (°C)		
DT (OD05)	69.95	0.045	7	1	10–200	25	116.59	This study
Jordanian DT	27.80	–	11	48	100–1000	20	198	[42]
Egyptian DT (Masakheet)	–	–	8	2	60–200	25	104.797	[43]
Marocco diatomite	22.7	–	7	0.3	8	RT	10.57	[40]
Beer brewery waste (DT waste, Celite Co., USA)	4.522	0.0317	7	24	0.5–2.5	25	4.92	[47]
DT (Celite Co., USA)	2.133	0.0045	7	24	0.5–2.5	25	1.80	[47]
Natural clay	30.0	–	5.65	1	10–100	20	58.2	[48]
Ghassoul (Morocco)	–	–	4.5–5	2	100–600	25	294	[46]
Kaolin (India)	–	–	–	3	10–25	27	13.99	[49]
Unmodified Zeolite	–	–	6.85	1	5–55	25	8.67	[50]
Raw clay (Benguerir, Marocco)	–	–	6.5	0.5	10–80	25	30	[51]
Phosphate naturel (Marocco)	–	–	–	3	–	25	7.46	[52]
Gypsum	5.67	–	7.5	1.5	5–25	25	36	[53]

RT, room temperature; DT, diatomite

When applied as an adsorbent for the methylene blue (MB) dye removal study, OD diatomite samples displayed good adsorption ability, evidencing good interactions between with MB dye adsorbate. The isotherm data fitted well the Langmuir model, and the calculated adsorption capacity of MB dye reached 116.59 mg/g (OD05) at 25 °C and pH 7.0. The obtained performances were comparable to those regarding several interesting materials reported in the literature.

These preliminary findings highlighted the potential use of the studied Ouled Djilali diatomite as promising low-cost and ecofriendly adsorbent for dyes separation from wastewater containing toxic contaminants. A conclusion can be also stated about the variation in diatomite characteristics, in the same deposit, with the variation in the geological layer or depth, fact which has to consider the suitable destination to choose for any industrial application.

Acknowledgements Authors would like to thank the “Ecole Nationale Supérieure des Sciences de la Mer et de l’Aménagement du Littoral” (ENSSMAL) laboratories and the « Centre de Recherche scientifique et technique en Analyses Physico-Chimiques » (CRAPC) for their cooperative support. We sincerely would like to extend our acknowledgments to the editors and the reviewers for their careful review contributing to improving the quality of this paper.

Compliance with ethical standards

Conflict of interest The authors declare that they have no conflict of interest.

Open Access This article is licensed under a Creative Commons Attribution 4.0 International License, which permits use, sharing, adaptation, distribution and reproduction in any medium or format, as long as you give appropriate credit to the original author(s) and the source, provide a link to the Creative Commons licence, and indicate if changes were made. The images or other third party material in this article are included in the article’s Creative Commons licence, unless indicated otherwise in a credit line to the material. If material is not included in the article’s Creative Commons licence and your intended use is not permitted by statutory regulation or exceeds the permitted use, you will need to obtain permission directly from the copyright holder. To view a copy of this licence, visit <http://creativecommons.org/licenses/by/4.0/>.

References

- Ma L, Chen Q, Zhu J, Xi Y, He H, Zhu R, Tao Q, Ayoko GA (2016) Adsorption of phenol and Cu (II) onto cationic and zwitterionic surfactant modified montmorillonite in single and binary systems. *Chem Eng J* 283:880–888. <https://doi.org/10.1016/j.cej.2015.08.009>
- Akti F (2018) Photocatalytic degradation of remazol yellow using polyaniline-doped tin oxide hybrid photocatalysts with diatomite support. *Appl Surf Sci* 455:931–939. <https://doi.org/10.1016/j.apsusc.2018.06.019>
- Namasivayam C, Prabha D, Kumutha M (1998) Removal of direct red and acid brilliant blue by adsorption onto banana pith. *Biore-sour Technol* 64:77–79
- Sharma YC, Upadhyay Uma SN, Gode F (2009) Adsorptive removal of a basic dye from water and wastewater by activated carbon. *J appl Sci in Environ Sanit* 4(1):21–28
- Lin SH, Juang RS (2009) Adsorption of phenol and its derivatives from water using synthetic resins and low-cost natural adsorbents: a review. *J Environ Manag* 90:1336–1349. <https://doi.org/10.1016/j.jenvman.2008.09.003>
- Yu F, Ma J, Wang J, Zhang M, Zheng J (2016) Magnetic iron oxide nanoparticles functionalized multi-walled carbon nanotubes for toluene, ethylbenzene and xylene removal from aqueous solution. *J Chemoph*. <https://doi.org/10.1016/j.chemosphere.2015.12.018>
- Cheng WP, Gao W, Cui X, Ma JH, Li RF (2016) Phenol adsorption equilibrium and kinetics on zeolite X/activated carbon composite. *J Taiwan Inst Chem Eng* 000(2016):1–7. <https://doi.org/10.1016/j.jtice.2016.02.004>
- Ouakouak A, Rihani K, Youcef L, Hamdi N, Guergazi S (2020) Adsorption characteristics of Cu (II) onto CaCl₂ pretreated Algerian bentonite. *Mater Res Exp*. <https://doi.org/10.1088/2053-1591/ab5ee4>
- Sarioglu M, Atay UA (2006) Removal of methylene blue by using biosolid. *Global NEST J* 8(2):113–120
- Tahir H, Sultan M, Jahanzeb Q (2008) Removal of basic dye methylene blue by using bioadsorbents *Ulva lactuca* and *Sargassum*. *Afr J Biotechnol* 7(15):2649–2655
- Gupta VK, Mohan D, Sharma S, Sharma M (2000) Utilization of Bagasse Fly Ash (a sugar industry waste) for the removal of copper and zinc from wastewater. *Sep Purif Technol* 18:131–140
- Benaïssa H. (2008) Effect of pH on the removal of methylene blue from synthetic aqueous solution by a natural waste material: almond pee. *Sci Stud Res IX(2)*, ISSN 1582–540X.
- Bessedik M, Belkebir L, Mansour B (2002) Révision de l’âge miocène inférieur (au sens des anciens auteurs) des dépôts du bassin du Bas Chélif (Oran, Algérie): conséquences biostratigraphiques et géodynamiques. *Mémo Serv géolog d’Algérie* 11:167–186
- Mansour B, Bessedik M, Saint Martin J-P, Belkebir L (2008) Signification paléoécologique des assemblages de diatomées du Messinien du Dahra sud-occidental (bassin du Chélif, Algérie nord-occidentale). *Geodiversity* 30(1): 117–139 (annexes available on: www.geodiversitas.com).
- Moret L (ed) (1964) Manuel de paléontologie végétale. Masson et Cie, Paris
- Hamdi B (1998) Etude physico-chimique de la surface des diatomites, Thèse de doctorat d’état en science .U.S.T.H.B, Algérie
- He Y, Jiang DB, Jiang DY, Chena J, Zhang YX (2018) Evaluation of MnO₂-templated iron oxide-coated diatomites for their catalytic performance in heterogeneous photo Fenton-like system. *J Hazard Mater* 344:230–240
- Wang Z, Lin Y, Wu D, Kong H (2016) Hydrous iron oxide modified diatomite as an active filtration medium for phosphate capture. *Chemosph* 144:1290–1298
- Rabbani M, Rafiee F, Ghafuri H, Rahimi R (2016) Synthesis of Fe₃O₄ nanoparticles via a fast and facile mechanochemical method: modification of surface with porphyrin and photocatalytic study. *Mater Lett* 166: 247–250. Doi: <https://doi.org/10.1016/j.matlet.2015.12.087>
- Barbosa IA, Zanatta LD, Espimpolo DM, Silva DL, Nascimento LF, Zanardi FB, Sousa Filho PC, Serra OA, Iamamoto Y (2017) Magnetic diatomite (Kieselguhr)/Fe₂O₃/TiO₂ composite as an efficient photo-Fenton system for dye degradation. *Solid State Sci* 72(2017):14–20

21. Rouchy JM, Caruso A, Pierre C, Blanc-Valleron MM, Bassetti MA (2007) The end of the Messinian salinity crisis: evidences from the Chelif Basin (Algeria). *Palaeogeogr Palaeoclimatol Palaeoecol* 254:386–417
22. Perrodon A (1957) Etude géologique des bassins néogènes sublittoraux de l'Algérie occidentale. Pub. Serv. Carte géol. Algérie, n. s. Alger, Bull. 12,382p.
23. Langmuir I (1918) The adsorption of gases on plane surfaces of glass, mica and platinum. *J Am Chem Soc* 40(1918):1361–1367
24. Freundlich HMF (1906) Über die adsorption in losungen. *Z Phys Chem (Leipzig)* 571:385–470
25. Sips R (1948) The structure of a catalyst surface. *J Chem Phys* 16:490–495
26. Temkin M.I. (1941) Adsorption equilibrium and the kinetics of processes on nonhomogeneous surfaces and in the interaction between adsorbed molecules. *Russian J Phys Chem (USSR)* 15:296–332
27. Eltaweil AS, Elshishini HM, Ghatass ZF, Elsubruiti GM (2020) Ultra-high adsorption capacity and selective removal of Congo red over aminated graphene oxide modified Mn-doped UiO-66 MOF. *Powder Technol.* <https://doi.org/10.1016/j.powtec.2020.10.084>
28. Eltaweil AS, Elgarhy GS, El-Subruiti GM, Omer AM (2020) Carboxymethyl cellulose/carboxylated graphene oxide composite microbeads for efficient adsorption of cationic methylene blue dye. *Int J Biol Macromol* 154:307–318
29. Fu X, Liu Z, Wu B, Wang J, Lei J (2016) Preparation and thermal properties of stearic acid/diatomite composites as form-stable phase change materials for thermal energy storage via direct impregnation method. *J Therm Anal Calorim* 123:1173–1181. <https://doi.org/10.1007/s10973-015-5030-1>
30. Yuan P, Wu DQ, He HP, Lin ZY (2003) The hydroxyl species and acid sites on diatomite surface: a combined IR and Raman study. *Appl Surf Sci* 227:30–39. <https://doi.org/10.1016/j.apsusc.2003.10.031>
31. Inchaurrenondo N, Font J, Ramos CP, Haur P (2016) Natural diatomite: efficient green catalyst for Fenton-like oxidation of Orange II. *Appl Catal B Environ* 181:481–494. <https://doi.org/10.1016/j.apcatb.2015.08.022>
32. Badii K, Ardejani FD, Sabri MA, Limaee NY, Shafaei SZ (2010) Adsorption of acid blue 25 dye on diatomite in aqueous solution. *Indian J Chem Technol* 17:7–10
33. Benkacem T, Hamdi B, Chamayou A, Balard H, Calvet R (2016) Physicochemical characterization of a diatomaceous upon an acid treatment: a focus on surface properties by inverse gas chromatography. *Powder Technol* 294(2016):498–507. <https://doi.org/10.1016/j.powtec.2016.03.006>
34. Zhang S, Cui M, Zhang Y, Yu Z, Meng C (2016) Synthesis of zeolite Y from diatomite and its modification by dimethylglyoxime for the removal of Ni(II) from aqueous solution. *J Sol-Gel Sci Technol* 80:215–225. <https://doi.org/10.1007/s10971-016-4080-6>
35. Vassileva P, Gentscheva G, Ivanova E, Tzvetkova P, Voykova D, Apostolova M (2011) Characterization of natural diatomites from Bulgaria. *Compt Rend Acad Bulg Sci* 64-N06–2011. <https://www.researchgate.net/publication/280577650>.
36. Yu ZH, Zhang YF, Zhai SR, Wang Y, Pan YZ, Meng CG (2015) Amino-modified mesoporous sorbents for efficient Cd (II) adsorption prepared using non-chemical diatomite as precursor. *J Sol-Gel Sci Technol* 78:110–119. <https://doi.org/10.1007/s10971-015-3933-8>
37. Khraisheh MAM, Al-degs YS, Mcminn WAM (2004) Remediation of wastewater containing heavy metals using raw and modified diatomite. *Chem Eng J* 99:177–184
38. Eltaweil AS, Ali Mohamed H, Abd El Monaem EM, El Subruiti GM (2020) Mesoporous magnetic biochar composite for enhanced adsorption of malachite green dye: characterization, adsorption kinetics, thermodynamics and isotherms. *Adv Powder Technol.* doi: <https://doi.org/10.1016/j.apt.2020.01.005>
39. Ibrahim S-S, Selim A-Q (2010) Producing a micro-porous diatomite by a simple classification calcination process. *J Ore dress* 12(23):24–32
40. Ababou N, Meziane D, Kherbeche A, Chaqroune A (2002) Etude de l'adsorption de colorants textiles sur une diatomite marocaine. *Phys Chem News* 6:130–134
41. Zaitan H, Feronnato C, Bianchi D, Achak O, Chafik T (2006) Etude des propriétés texturales et adsorbantes d'une diatomite marocaine: Application au traitement D'air chargé d'un polluant de type composé organique volatil. *Annal Chim Sci Matér* 31(2):183–196
42. Al-Ghouti MA, Khraisheh MAM, Allen SJ, Ahmad MN (2003) The removal of dyes from textile wastewater: a study of the physical characteristics and adsorption mechanisms of diatomaceous earth. *J Environ Manag* 69:229–238
43. Mohamed EA, Selim AQ, Zayed AM, Komarneni S, Mobarak M, Seliem MK (2018) Enhancing adsorption capacity of Egyptian diatomaceous earth by thermo-chemical purification: methylene blue uptake. *J Colloid Interface Sci* 534:408–419. <https://doi.org/10.1016/j.jcis.2018.09.024>
44. Giles CH, Smith D, Huitson A (1974) A general treatment and classification of the solute adsorption isotherm I. Theoretical. *J Colloid Interface Sci* 47(3):755–765
45. Fröhlich AC, Ocampo-Pérez R, Diaz-Blancas V, Salau NPG, Dotto GL (2020) Three-dimensional mass transfer modeling of ibuprofen adsorption on activated carbon prepared by sonication. *Chem Eng J* 341:65–74. <https://doi.org/10.1016/j.cej.2018.02.020>
46. Ellass K, Laachach A, Alaoui A, Azzi M (2010) Removal of methylene blue from aqueous solution using ghasoul, a low-cost adsorbent. *Appl Ecol Environ Res* 8(2):153–163
47. Tsai W-T, Hsu H-C, Su T-Y, Lin K-Y, Lin C-M (2008) Removal of basic dye (methylene blue) from wastewaters utilizing beer brewery waste. *J Hazard Mater* 154:73–78
48. Gürses A, Doğar Ç, Yalçın M, Açıkıldız M, Bayrak R, Karaca S (2006) The adsorption kinetics of the cationic dye, methylene blue, onto clay. *J Hazard Mater B* 131:217–228.
49. Ghosh D, Bhattacharyya K-G (2002) Adsorption of methylene blue on kaolinite. *Appl Clay Sci* 20:295–300
50. Jin X, Jiang M, Shan X, Pei Z, Chen Z (2008) Adsorption of methylene blue and orange II onto unmodified and surfactant-modified zeolite. *J Colloid Interface Sci* 328:243–247
51. Allam K, Gourai K, El Bouari A, Belhorma B, Bih L (2018) Adsorption of Methylene Blue on raw and activated Clay: case study of Bengurir clay. *J Mater Environ Sci* 9(6):1750–1761. <https://doi.org/10.26872/jmes.2018.9.6.195>
52. Barka N, Nounah A, Assabbane A, Aitichou Y (2006) Evaluation du pouvoir adsorbant du phosphate naturel dans le traitement des rejets textiles: comparaison avec le charbon actif. *Proc Covaphos II* 4:195–203
53. Muhammad AR, Shehadeh I, Ahmed A, Al-Zamly A (2009) Removal of methylene blue from aqueous solution by using gypsum as a low cost adsorbent. *World Acad Sci Eng Technol* 55:608–613

Publisher's Note Springer Nature remains neutral with regard to jurisdictional claims in published maps and institutional affiliations.